



RESEARCH ARTICLE

Production of industrial hemp (*Cannabis sativa*) plant added PA66 nanofiber membranes by the electrospinning method: Investigation of water desalting performances

Abdullah Gü1*, Ismail Tiyek2,3, Ahmet Karadağ1 & Ibrahim Kılıç1

¹Hemp Research Institute, Yozgat Bozok University, Yozgat 66100, Türkiye

²Department of Textile Engineering, Kahramanmaraş Sutcu Imam University, Kahramanmaraş 46100, Türkiye

³Kahramanmaraş Sütçü Imam University, University-Industry-Public Collaboration, Research-Development-Application Centre, Kahramanmaraş 46100, Türkiye

*Correspondence email - abdullahgul46@gmail.com

Received: 12 March 2025; Accepted: 01 June 2025; Available online: Version 1.0: 17 June 2025

Cite this article: Abdullah G, Ismail T, Ahmet K, Ibrahim K. Production of industrial hemp (*Cannabis sativa*) plant added PA66 nanofiber membranes by the electrospinning method, investigation of water desalting performances. Plant Science Today (Early Access). <https://doi.org/10.14719/pst.8204>

Abstract

Clean water is a vital resource for humans, animals, agriculture, as well as industrial processes, which are the most widespread activities using the global resource. Desalination of seawater is a promising method to obtain abundant and reliable clean freshwater. It is a new nanotechnology application that attracts attention as a method to improve the performance by improving the surface properties to obtain nanofiber membranes for seawater desalination or desalination applications. Nowadays, polymeric nanofibers are one of the promising materials due to their significantly high permeability flux and selectivity, high porosity, properties. The industrial hemp (*Cannabis sativa*) plant is one of the important natural green fiber products. So far, there has been no insufficient research on hemp-doped membranes for water desalination and ion retention. This study focused on the fabrication of composite materials from polyamide-66-based nanofibers doped with hemp plant fibers in formic and acetic acid by the electrospinning method. SEM images showed an interconnected structure between PA66 and dissolved hemp plant fibers. Permeability properties and ion retention sensitivity studies of the filtration structure were performed. Contact angle study revealed its hydrophilic structure. This study can be a source of inspiration for researchers who can shed light on future research for hemp-doped nanofiber membranes, emphasizing sustainable development goals.

Keywords: electrospinning; hemp plant fiber; membrane; nanofiber; polyamide-66

Introduction

The fresh water scarcity that occurs in many regions as a result of world economic, urbanization and industrialization every year, will increase the billions of living creatures accumulated, especially in Africa and the Middle East. According to the 2022 reports of the World Health Organization (WHO), approximately more than 2.2 billion people do not have access to safe drinking and hygienic fresh water (1). Every year, approximately 3 million people are seriously affected and may even die by unsafe and contaminated water sources. Additionally, lack of access to clean water has led to approximately 50 % of total hospital beds being occupied by people suffering from related diseases (2-4). Many countries face serious problems in this regard. Various technological methods, such as desalination, have given hope to people in water-scarce regions. Among the biggest environmental challenges faced today, water scarcity is one of the most critical and rapidly emerging problems. This situation may become even more serious when the limitations in the availability of freshwater resources around the world are highlighted. Although

approximately 97 % of the Earth is covered with water, it is too salty to be used for drinking, irrigation or industrial purposes. Therefore, only 3 % of the available water can be used by humans and other living creatures such as livestock and poultry (5).

Membrane desalination is an effective technology that produces fresh water from brackish water or seawater using nanofiltration (NF) membrane processes (6). Although porous semipermeable membranes are generally obtained from many polymers, cellulosic polymers, aromatic polyamides (PAs) and polysulfones (PSFs) are the most preferred polymer materials for today's desalination and water purification technologies (7). Despite increasing interest in desalination membranes with improved chemical resistance and thermal stability, the separation performance of newly reported membrane material is generally measured by water flux and salt rejection. While high flux and high rejection are goals pursued by membrane scientists, both flux and salt retention testing are easily affected by salt feed concentration, membrane thickness and operating pressure and cannot accurately reflect the inherent desalination performance of polymer membrane materials (8). Research into the

development of sustainable polymeric composite membranes has attracted increasing academic and industrial interest in recent years due to modern society's increasing demand for accountable high-performance materials and more environmentally conscious consumers, industries and governments.

Electrospinning technology has attracted great attention in recent years due to its ability to continuously and uniformly obtain sub-micron and nanometer diameter fibers. Unlike traditional phase transformation membranes or melt-spinning stretch membranes, electrospinning technology can offer membranes with significantly higher porosity (up to 90 %), relatively uniform pore size distribution, high interconnectivity of pores, controllable pore size and large specific surface area. As a result, electrospinning technology has attracted widespread attention in the preparation of functional membranes, showing great potential in filtration and separation, biomedical-energy and many other fields (9).

PA66 membranes are the most common membranes used in nanofiltration and desalination due to their high permeability and excellent thermal and mechanical properties (10). PA66 has excellent chemical stability and thermal resistance. It is usually dissolved in formic acid and from there it can be easily converted into nanofibers (11). PA66 membranes are characterized by high permeability and filtration efficiency, making them the most widely used membranes in practical applications (12).

Hemp has great potential for versatile applications. The cannabis plant (*Cannabis sativa* L.) is one of the world's oldest crops, widely grown for industrial (13), food (14), medicinal and psychoactive (15) uses. Hemp, if managed correctly, is a highly sustainable and ecologically benign crop that directly serves the European Green Deal and the Circular Economy Action Plan. Industrial hemp is of interest for agriculture, pharmaceutical, food, textile, construction and other industries and the inherent mechanical, thermal and acoustic properties of its fibers make it promising components for reinforcements in polymer composite materials (16).

Based on these existing studies, in this study, we embark on a new journey to obtain and illuminate hemp fiber-reinforced PA66-based membrane surfaces using the electrospinning method, one of the most effective methods in nanofiber production. With the qualified outputs obtained, we have a comprehensive understanding that sheds light on the literature and closes the existing knowledge gap. The purpose of this study is to provide information that can shape the future course of hemp-reinforced membrane applications.

Material and Methods

Materials

PA66 pellet (Formula Weight: 262.36 g/mol, Density: 1.19 g/mL), formic acid (HCOOH, >98 %), sodium hydroxide pellet (NaOH >98 %), hydrochloric acid (HCl, 37 %) and acetic acid (CH₃COOH, 100 %) were obtained from Sigma Aldrich. Hemp plant fiber (HF) plant was obtained from Yozgat Bozok University Hemp Research Institute in Turkey.

Methods

Preparation of hemp fibers

First, hemp plant fibers were chemically pretreated (cleaning and bleaching) to reduce hemicellulose and lignin content. Pretreatment is usually done with sodium hydroxide (NaOH) to remove lignin and pectin found in the hemp fiber plant (17-19). In this study, firstly, 2 % NaOH aqueous solution was prepared and then the hemp bast fiber mixture was autoclaved at 121 °C for 1 hr. Then, after neutralization with 37 % HCl, the mixture was washed 3 times with distilled water and filtered. After the upper part of the mixture was discharged to room temperature and the precipitated fibers were dried, it was kept in the oven at 50 °C for 1 day. After chemical pretreatment, hemp fibers were ground into small pieces (0.1-2 mm) with a ball mill for better dissolution.

Preparation of hemp-added solution

To be used in the production of nanofiber membranes, solutions containing PA66 and HF in different mixing ratios were prepared with a total solid content of 10 % by weight. For this purpose, 5 different solutions were prepared by adding different ratios of PA66/HF (100/0, 99/1, 96/4, 92/8 and 90/10 by weight). The products are named HF-0, HF-1, HF-4, HF-8 and HF-10, respectively. The mixing ratios of HF added to the PA66 solution are given in Table 1. Formic acid and acetic acid were used as solvents in a ratio of 3:1. Each solution was first mixed in a heated magnetic stirrer at 50 °C for 30 min and then at room temperature for 12 hr. These solutions were finally processed in an ultrasonic bath for 30 min at room temperature.

Table 1. Mixing ratios of HF added to the PA66 solution

Kode	Total solids content (%)	PA66 (%)	HF (%)
HF-0		100	0
HF-1		99	1
HF-4		96	4
HF-8	10	92	8
HF-10		90	10

Electrospinning device and working process

Performed on NanoSpinner. PilotLine model semi-industrial multi-nozzle electrospinning device (Fig. 1) is located at Kahramanmaraş Sütçü İmam University (KSÜ) Materials Research Laboratory at USKIM. While spinning the solutions from the device, parameters such as power, feed and needle tip-collector distance were determined precisely. The working process was carried out at a distance of 195 mm, a feed rate of 0.4 ± 0.1 mL/h and a voltage of 29 kV. In addition, each study was carried out at a winding speed of 10 (cm/min) for 50 times. The prepared polymer solutions were drawn into a 10 mL plastic syringe and then placed into the device. White polypropylene spunbond nonwoven fabric with a weight of 12 g/m² and a width of 48 cm was used as the base material in the electrospinning device.

SEM analysis

The surface morphologies of the produced PA66/HF composite membranes were analyzed using a scanning electron microscope (SEM), ZEISS brand EVO/LS10, at Yozgat

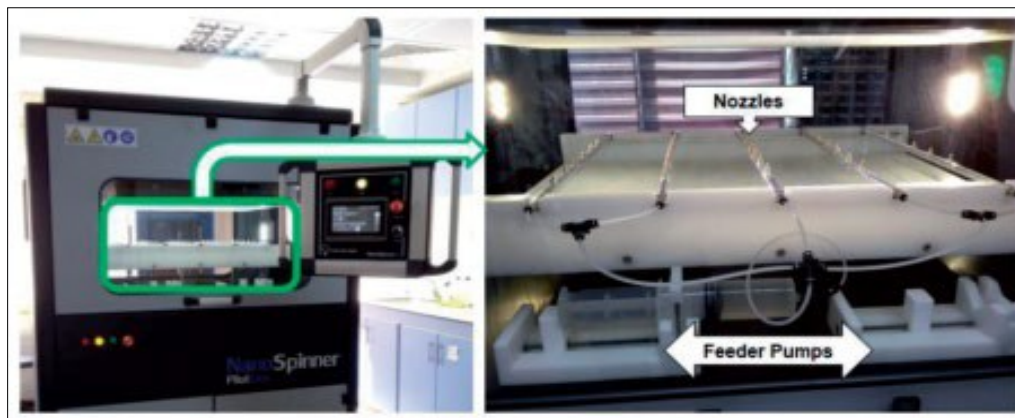


Fig. 1. INOVENSO semi-industrial multi-nozzle electrospinning device.

Bozok University BILTEM laboratories. To obtain higher yield data from the analyses, the samples were coated with a thin gold layer on a gold coating device (Cressington 108 auto device) before SEM analysis. For each sample, X1000, X5000, X10000 and X20000 magnification parts were examined, but only 20 different fiber diameter measurement studies were shared in 2000 magnification images.

Contact angle test measurements

KSV Attension brand Theta model contact angle measuring device was used. The measurement technique used in this device is the method of dropping ultrapure water onto the membrane sample surface. Contact angle test measurements were performed on the surface of dry membrane samples. As a method, at least 10 measurements were made for each membrane sample.

Dead-end mixing cell filtration process

The performance tests of the membranes obtained by the electrospinning method against pure water and salt water were performed. Pure water flux was measured using the dead-end mixing cell filtration system mentioned above. The membrane was pre-compressed at 0.6 bar applied pressure until a constant water flux was obtained. Water flux at 25 °C was measured at 0.6 bar applied pressure. The following equations were used to calculate the hydraulic permeability of the membrane. The characteristics of the vacuum membrane filtration system used are given in Table 2.

Table 2. Technical information of vacuum filtration system

Technical data	Technical value
Filter Membrane Area (m ²)	0.00138
Maximum Filter Volume (mL)	250
Filter Vacuum Value (Bar)	0.6

The performance tests of the membranes

The performance tests of the membranes obtained by the electrospinning method were carried out by measuring the permeability of pure water and salt water (containing NaNO₃) using a vacuum membrane filtration system. The pressure filtration cell shown in Fig. 2 was used to determine the permeability values of the produced membranes for pure water and 0.4 M NaNO₃. Before the permeability experiments, the produced membranes were immersed in pure water for 120 min at room temperature. The purpose of the wetting process is to prepare the membrane nanofibers for the

process before the membrane flux process. After the wetting process, the flux at 0.6 bar pressure was calculated according to Eqn. 1. The permeability values were determined using the calculated flux value. Each sample was processed 10 times and the average values were considered (20).

$$J_w = V / (A \times \Delta t) \quad (1)$$

Here;

J_w is calculated as flux (L/m²·h), V is calculated as permeation volume (L), A is calculated as membrane active area (m²) and Δt is calculated as time (hr).

Permeability value (Eqn. 2);

$$\text{Permeability} = J_w / P \text{ (L/(m}^2\text{-h-bar}) \quad (2)$$

It is obtained with the formula (20).

The air permeability test of the membrane samples was carried out in the PROWHITE Air Test-2 device located in the physical examination laboratory of the Textile Technologies Department of the Technical Sciences Vocational School of KSU. The test samples were prepared with an area of 20 cm² and were carried out at an air pressure of 100 ± 10 Pa. Five test procedures were carried out for each test sample and their average values were considered.

In this study, the average pore size (r_m) (Eqn. 3) was calculated with the filtration rate using the Guerout Elford-Ferry equation (20-22).

$$\sqrt{\frac{(2.9 - 1.75\epsilon) \times 8\eta lQ}{\epsilon A \Delta P}} \quad (3)$$

Here;

ϵ : Membrane porosity ratio (%),

η : Viscosity value of pure water (8.9×10^{-4}),

i : Membrane thickness (m),

Q : Permeable volume per unit time,

A : Effective area of the membrane,

ΔP : Applied bar (Mpa).

Also in this study, the gravimetric method based on the weight of the liquid in the membrane pores was preferred to calculate the membrane porosity ratio (ϵ), which is the ratio of the pore volume of the membranes to the membrane geometric volume (Eqn. 4) (23-26).

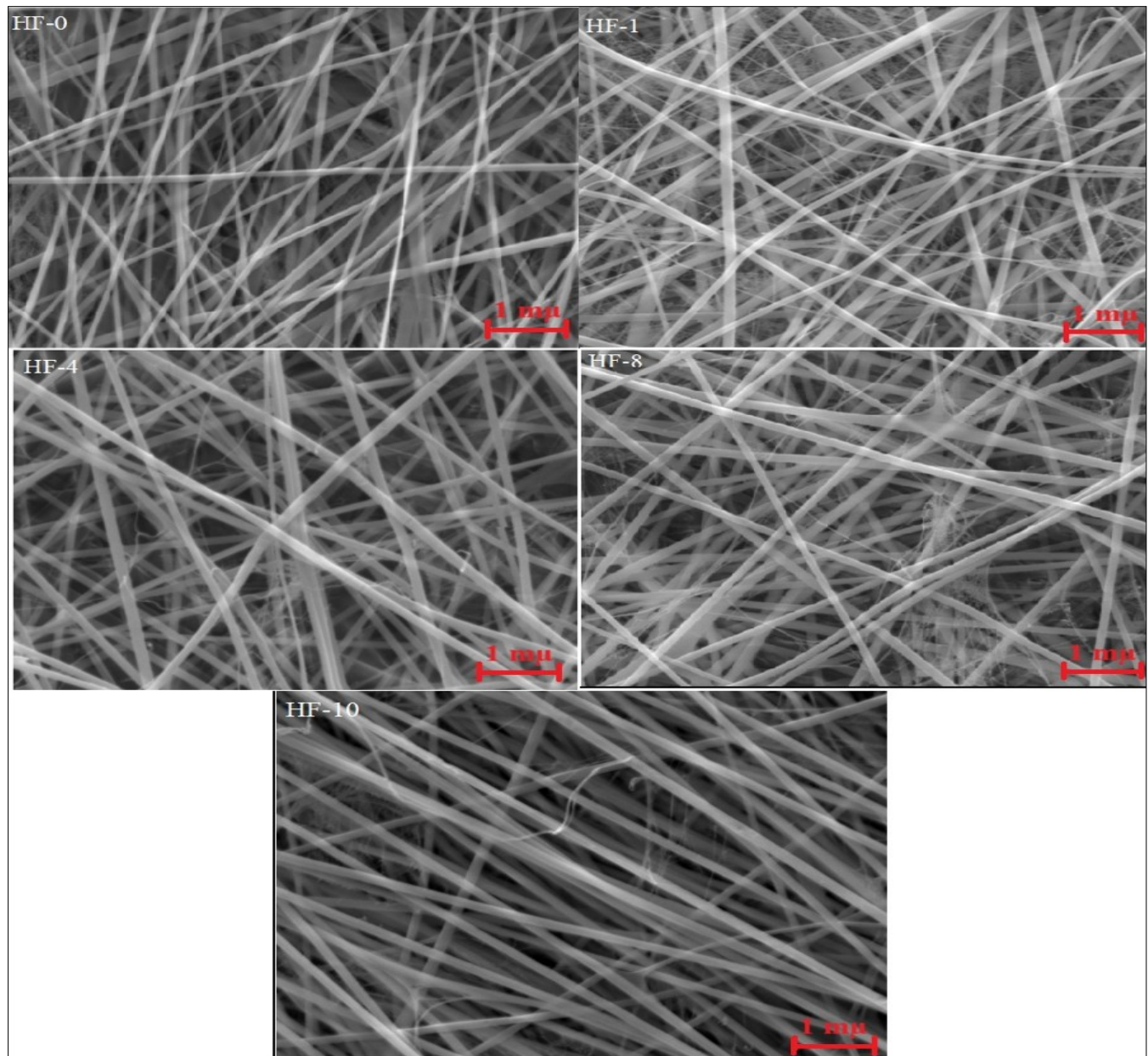


Fig. 2. SEM images of fiber at $\times 20000$ magnification.

$$\varepsilon(\%) = \frac{W_w - W_d}{AL\rho} \times 100 \quad (4)$$

Here;

W_w : Wet weight of the membrane (g),

W_d : Dry weight of the membrane (g),

A : Area of the sample (cm^2),

L : Average thickness of the sample (cm),

ρ : Density of pure water (0.998 g/cm^3).

In the study, the ion retention performances of the produced membranes were analyzed using 0.6 bar pressure and 0.4 M NaNO_3 salt solution. At this pressure value, the salt permeability values of the ionic salt solutions were calculated using Eqn. 5. For salt removal rates, the conductivity values of the filtrate and fed solutions were measured in mV and the ion removal rates were expressed as % using Eqn. 5 (27, 28). Three separate studies were performed for each sample and the average value was considered.

$$R(\%) = \frac{C_f - C_p}{C_f} \quad (5)$$

In the formula, R represents the retention (%), C_f represents the electrical conductivity values of the feed solution and C_p represents the electrical conductivity values of the filtrate solution.

Measurement of swelling property

The swelling properties of the membrane samples were tested in 50 mL of phosphate salt buffer (pH 1.0 and 37 °C). It was kept for 15, 30, 45 and 60 min. Then, surface water was removed with moistened towel paper and the samples were weighed at predetermined time intervals. Dry and wet weights were recorded and put into the percentage swelling equation (%SD). The degree of swelling (SD) of the membranes was calculated by the following Eqn. 6 (43).

$$\text{SD}(\%) = [(M_t - M_0)/M_0] \times \% 100 \quad (6)$$

In the formula, M_t : weight of wet membrane, M_0 : weight of dry membrane.

Results and Discussion

Solution characterization studies

The operating parameters and system requirements for the electrospinning manufacturing process can vary greatly depending on the choice of polymer and solvent. The density, viscosity and conductivity of the solution are critical factors that affect the spinnability of the solution as well as the morphology of the spun fibers (30).

Table 3 shows that as the hemp content in hemp-doped PA66 solutions increases, the solution viscosity increases significantly, whereas the solution conductivity decreases slightly (31, 32).

Table 3. Density, conductivity and viscosity values of solutions

	Density (gr/cm³)	Conductivity (ms/S)	Viscosity (cP)
HF-0	1.112	401	701
HF-1	1.139	381	812
HF-4	1.142	370	1115
HF-8	1.162	350	1178
HF-10	1.198	346	1512

Morphological analysis

To verify the aggregation effect on hemp fibers in hemp-doped PA66 polymer solution, the morphology of hemp fibers before and after doping was observed by scanning surface electron microscopy. It was found that the microstructure of hemp-doped and doped nanofiber samples exhibited fiber diameters with a diameter in the nanometer scale. Fig. 2 shows the SEM images of the fiber diameter distribution of nanostructured fibers obtained by electrospinning from hemp-doped and non-doped PA66 polymer at different mixing ratios at $\times 20000$ magnification. Table 4 shows the diameter measurement values of the fibers. From the shared images, all samples have a distinct fibrous structure and the obtained surfaces prove that a bead-free and nanostructured fibrous membrane surface can be produced.

The average fiber diameter of the nanofibers obtained from the hemp-free PA66 polymer is approximately 124 nm, while it is seen that problem-free, randomly oriented fibers are obtained. However, with increasing ratios, the average fiber diameter of the hemp weft nanofibers was determined to be approximately 140, 160, 167 and 172 nm, respectively, depending on the additive ratio. It was determined that the fiber diameter value increased significantly with the increase of the hemp additive ratio. The increase in the average diameter of the nanofibers can be explained by the fact that the viscosity of the hemp added to the PA66 solution increases the viscosity of the PA66 solution and as a result, the same thing happens when there is a certain amount of hemp added to it. However, we can also explain this by determining the decreasing conductivity value depending on the hemp doping ratio (29). It was understood that as the amount of hemp fibers in the PA66 polymer solution increased, they all exhibited a smooth fiber structure depending on the spinning viscosity. As a result, it was determined that the addition of hemp fibers to the PA66 polymer solution did not have a great effect on the spinning process and that problem-free and bead-free fibers could be obtained.

Table 4. Fiber diameter values of nanostructured fibers

	Density (nm)
HF-0	124 \pm 34
HF-1	140 \pm 61
HF-4	160 \pm 72
HF-8	167 \pm 40
HF-10	172 \pm 50

The histogram of fiber diameter (Fig. 3) clearly shows that fibers with increasing diameter are produced within a narrow range as the hemp content in the PA66 polymer solution increases. These results indicate that the diameter of the fibers can be controlled simply by changing the bulk compositions of the component polymers.

Contact angle

Contact angle analysis was performed to determine the hydrophobic and hydrophilic characteristics of the obtained membranes and is shared in Fig. 3. It is known that the PA66 polymeric membrane surface without hemp additive has a relatively hydrophobic surface. However, it is observed that the hemp-added PA66 polymeric membrane surfaces gain a hydrophilic structure depending on the hemp additive ratio (34). This may be related to the presence of a significant number of hydrophilic groups in PA66 and the fact that the hydrophilic groups become dominant on the surface as the lignocellulosic hemp is distributed homogeneously in the mixing system (35). The hydrophilic structure of the membrane material shows that it is less resistant to the passage of water. In addition, the wettability of the surface prevents bacteria and organic substances from adhering to it and contributes to the ability to be washed more easily.

Most importantly, water molecules bind to the hydrophilic membrane surface via hydrogen bonds, forming a thin water barrier between the membrane surface and the permeable solution. This acts as a boundary that prevents the residues of unwanted hydrophobic membrane contaminants on the membrane surface (36). The presence of hydrophilic surfaces in membrane structures is expressed as an important factor in improving antimicrobial agent loading and antimicrobial performance. The membranes with hydrophilic surfaces can load more antimicrobial agents and show higher antimicrobial performance than hydrophobic surfaces were explained (37). Therefore, hemp-doped PA66 composite membrane is expected to offer promising potential in antimicrobial agent loading.

Water flow and permeability

In the permeability performance tests of hemp-added PA66 nanofiber membranes obtained with Eqn. 1 and 2, the effect of two different flux values (water and salt water) on nanofiber membrane performance is given in Fig. 4.

When the obtained results are evaluated, it is seen that as the hemp weight percentage increases, there is a decrease in pure water and salt water flux values. In addition, the permeability value decreases visibly under 0.6 bar pressure. When the permeability values are examined, it is seen that the best pure water permeability value belongs to the HF-10 sample.

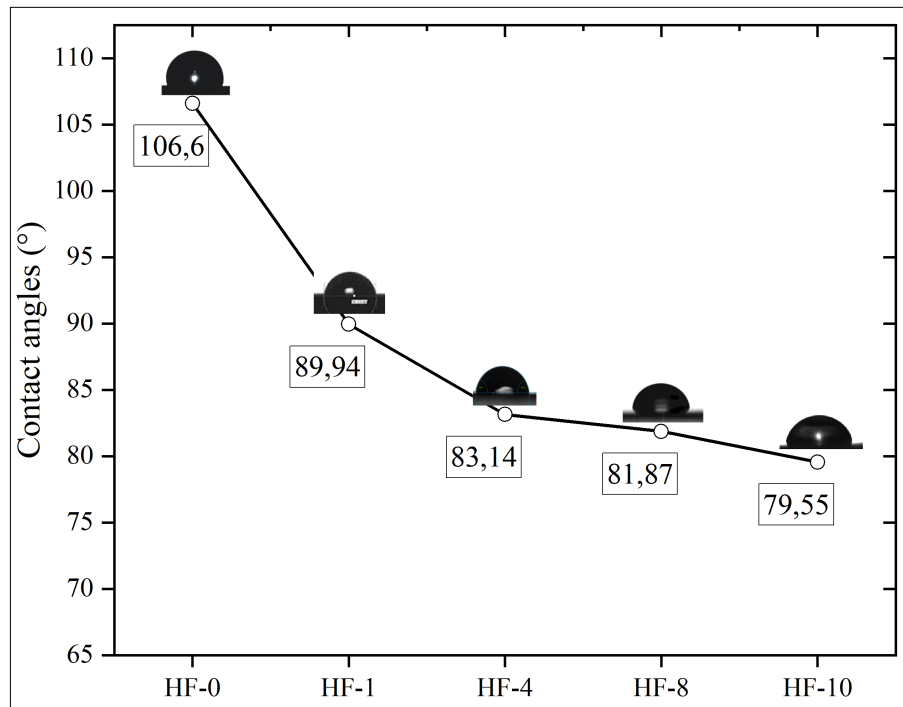


Fig. 3. Contact angle analysis of membranes.

The results showed that as the mass fraction of hemp in PA66 increased the flux through the membrane decreased. As the amount of hemp in the polymeric solution increased, the voids along the cross-section of the membrane were filled. In addition, the nanofiber with a higher amount of hemp added increased the surface roughness, resulting in greater adhesion of water droplets on the membrane surface and the formation of a resistant layer that could prevent hemp from contacting the surface water, thus leading to an overall decrease in flux. Lignocellulosic membrane material also swells when exposed to water (38, 39). The swelling of the polymer reduces the overall porosity of the membrane. As a result, it forms a compact structure with less porosity and ultimately less flux. Fig. 4(A, B) shows that both flux and permeability decrease with the hemp flux rate, respectively. It was observed that the membrane hydrophilicity trend is in strong agreement with the permeability and flux trends (42).

In general, we see in literature studies that flux and permeability values are related to membrane nanofiber

diameter and porous structure and are also proportional to membrane thickness values. In this context, it is generally observed that the flux value increases as membrane thickness increases (40). In addition, these results confirm that flux decreases as the contact angle decreases. This confirms that the hydrophilic structure also decreases gradually. Rana and colleagues argued that all three concepts are related to each other. In the literature, the rapid decrease in flux is attributed to the decrease in membrane porosity (41). The increase in flux value as the hemp ratio in the solution concentration increases can be explained by the hydrophilic structure of lignocellulosic doped membrane structures.

Pore ratio and pore size analyses

The porosity of the membranes was measured by the gravimetric method and the average pore sizes of the membranes were calculated by Guerout-Elford-Ferry (Eqn. 4) based on pure and salt water flux data (Fig. 5).

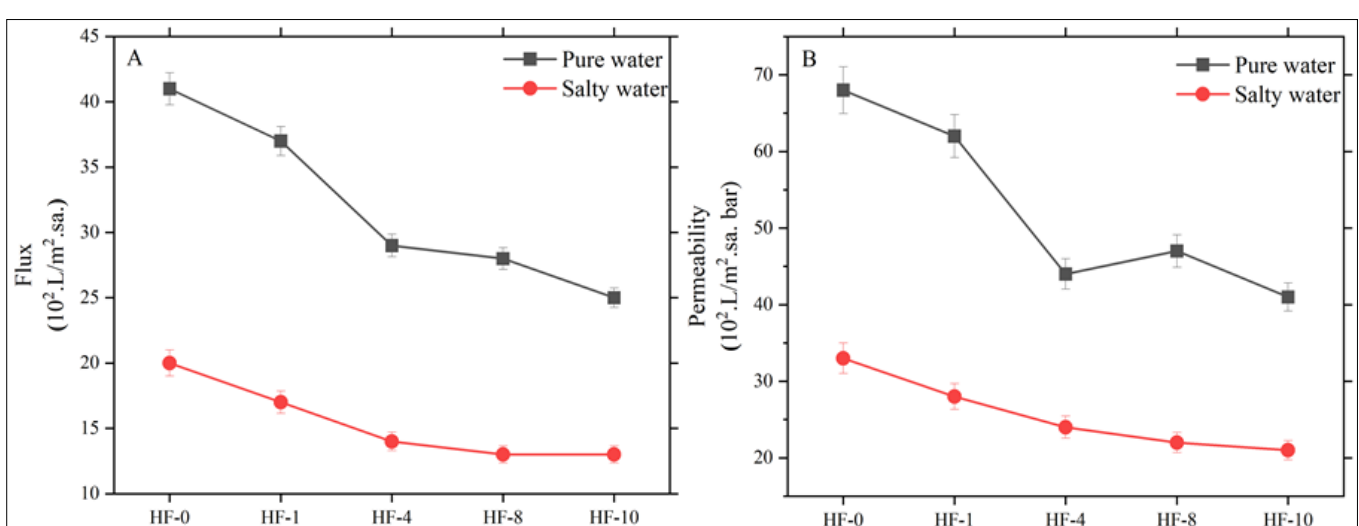


Fig. 4. Flux (A) and permeability (B) performance test graphs of hemp-doped PA66 nanofiber membranes.

The pore size of the nanofiber-structured HF-0 membrane surface obtained without hemp additive was calculated as an average of 60 % using Eqn. 3. It was determined that the porosity of the surfaces decreased due to the porous structure of the PA66 nanofiber membrane surfaces with increasing hemp additives depending on the weight percentages. It was determined that the porosity decreased by approximately 20 % in the HF-10 sample. It was determined that the pore size of the HF-0 sample, which was 216 nm, decreased depending on the hemp additive rate and this value was calculated as 188 nm, decreasing by approximately 13 % for the HF-10 sample.

In Fig. 5, the results show that the average pore size decreases with decreasing fiber diameter and can be argued as evidence that nanofibers have a high surface area. This study also confirmed this thesis put forward by previous studies. In addition, the results showed that membranes with larger fiber diameters have a larger porous structure between the fibers. There are other studies in the literature supporting this statement (40). We can say that these decreases are due to the decrease in the diameter of nanostructured fibers.

These results show that hemp additive increases the permeability properties of the membranes.

It is seen in Fig. 6 that as the hemp contribution of the ion retention percentage increases in the aqueous solution prepared as 1 M in the presence of NaNO_3 , the ion retention efficiency of the membranes also increases.

A noticeable improvement in the ion exchange capacity of the nanofiber-structured membrane surfaces obtained by increasing the hemp mixture ratio in the polymer solution was detected. This can be attributed to the hydrophilic property of the hemp in the lignocellulosic structure, which causes more water adsorption in the prepared membrane and thus facilitates the transport of ions between the solution and the membrane phase. This increases the ion retention possibilities. The presence of hydroxyl groups in hemp causes the development of hydrogen and Van der Waals bonds through PA66 mixtures. As these electrostatic interactions increase, cross-linking occurs, which allows the adhesion of salt ions.

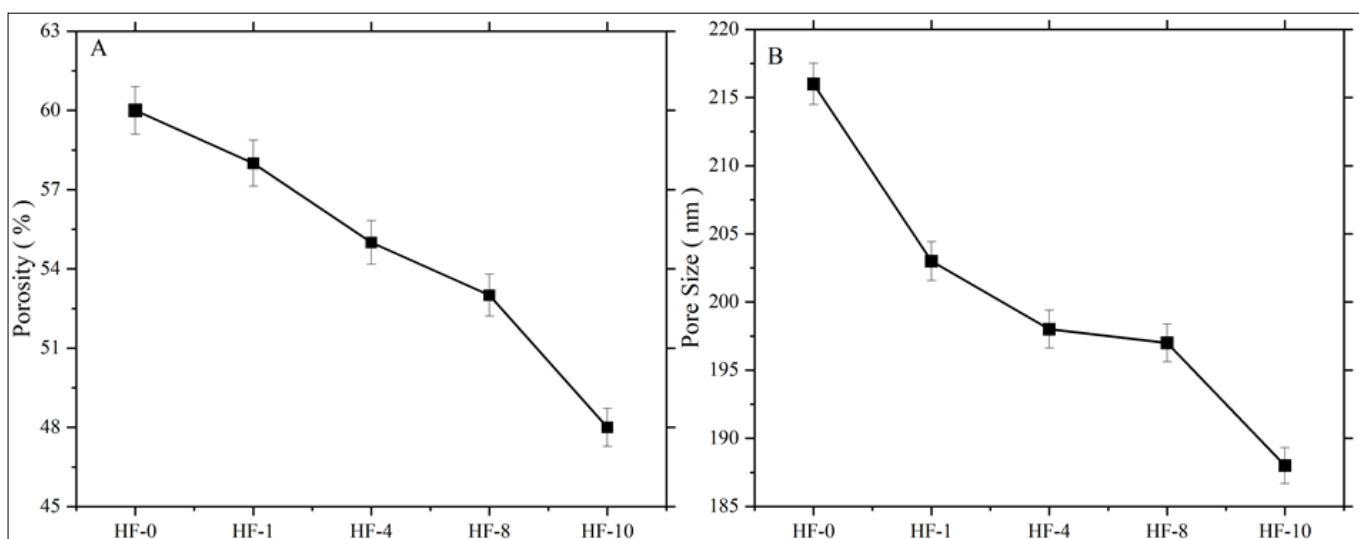


Fig. 5. Porosity (A) and pore size (B) performance test graphs of hemp-reinforced PA66 nanofiber membranes.

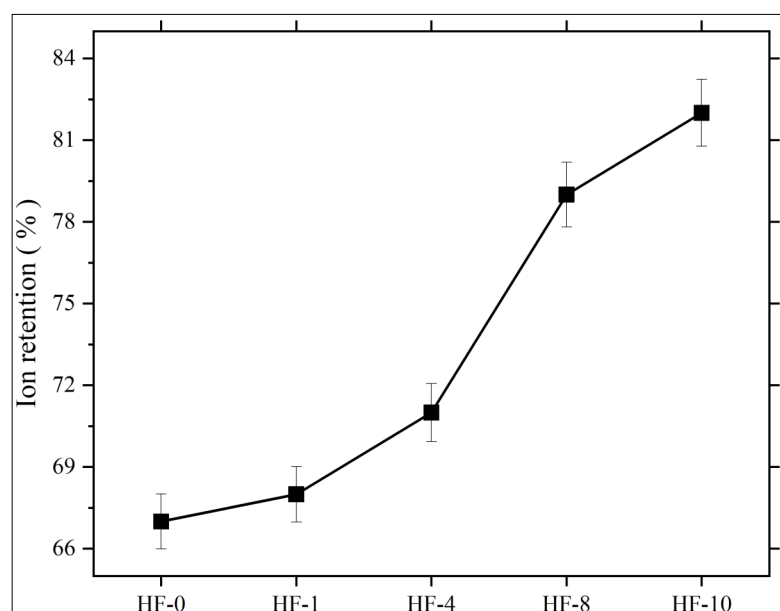


Fig. 6. Ion retention performances of hemp-doped PA66 nanofiber membranes.

Measurement of swelling property

Swelling test of membrane samples, percentage values depending on time are shared in Fig. 7. Swelling effect of cellulosic hemp on PA66 as seen in Fig. 7, the swelling ratio of nanofiber increased with the increase of hemp additive ratio. The negatively charged OH molecule of hemp contributes significantly to the absorption of water. The water absorption is caused by hydroxyl groups in cellulose and hemicellulose. Higher hydroxyl group content leads to higher water absorption and swelling coefficient (44). The results obtained showed that, depending on the fiber diameters, as the surface area increases, swelling increases along with the water absorption of the materials as a result of the roughness caused by hemp on the surface (45).

Conclusion

As a general result, an electrospinning process that will allow the production of membranes with uniform and homogeneous distribution by preparing a solution suitable for both PA66 and hemp-added polymer mixtures has been successfully carried out. The formation of nano-sized fibers was observed in the hemp-added PA66 polymeric nanofiber membranes obtained and a material that can be used for the filter was produced. We can understand this from the high filtration efficiency on the fiber diameters and the network structure that provides homogeneous distribution. As a result of these results and evaluations obtained depending on the material and method used, the study prepared with 10 % additive was the most ideal in terms of ion retention efficiency, while the average value of the nanofiber diameter was calculated as 172 nm. This value is the highest among the other membrane samples. This study also conducted market research on PA66 polymers used for cost analysis in obtaining membrane surfaces with a nanofiber structure. Considering that the

PA66 sales price is higher than the hemp sales price, it is possible to say that increasing the hemp ratio in the polymer ratio will create a more affordable membrane. All the results obtained can be said to be a study that can shed light on future scientific studies on water treatment and ion retention filtration applications, where hemp can provide filtration efficiency at high vacuum values with polymer additives (depending on the type and mixing ratios of the polymer).

Acknowledgements

This study was supported by Yozgat Bozok University Scientific Research Projects with project code FKA-2023-1158.

Authors' contributions

AG helped in conceptualization, investigation, data acquisition, funding acquisition, writing - original draft; IT, AK and IK performed methodology and data analysis.

Compliance with ethical standards

Conflict of interest: Authors do not have any conflict of interests to declare.

Ethical issues: None

References

1. Progress on household drinking water, sanitation and hygiene. World Health Organization; [Accessed 22 February 2025]. <https://washdata.org/reports/jmp-2023-wash-households>
2. Sanaeepur H, Amooghin AE, Shirazi MMA, Pishnamazi M, Shirazian S. Water desalination and ion removal using mixed matrix electrospun nanofibrous membranes: A critical review. Desalination. 2022;528(1):115350. <https://doi.org/10.1016/j.desal.2021.115350>

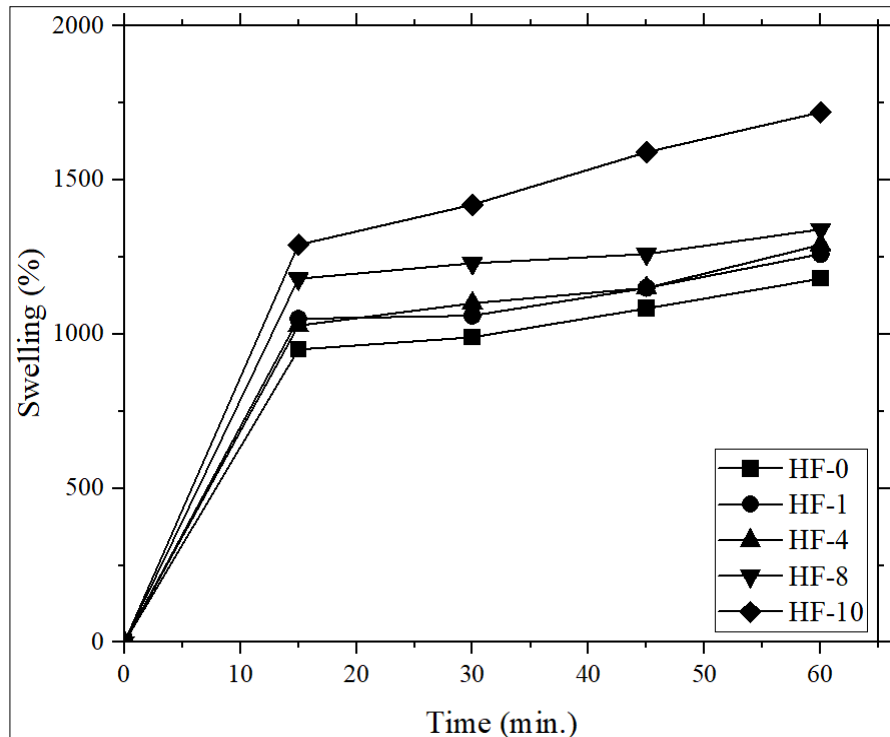


Fig. 7. Time-dependent swelling test of hemp-reinforced PA66 nanofiber membranes.

3. Eliasson J. The rising pressure of global water shortages. *Nature*. 2015;517:6. <https://doi.org/10.1038/517006a>
4. Pichel N, Vivar M, Fuentes M. The problem of drinking water access: A review of disinfection technologies with an emphasis on solar treatment methods. *Chemosphere*. 2019;218(1):1014-30. <https://doi.org/10.1016/j.chemosphere.2018.11.205>
5. Selatlie MK, Ray SS, Ojijo V, Sadiku R. Recent developments in polymeric electrospun nanofibrous membranes for seawater desalination. *RSC Adv.* 2018;8(1):37915-38. <https://doi.org/10.1039/C8RA07489E>
6. Ahmad AL, Ooi BS, Mohammad AW, Choudhury JP. Development of a highly hydrophilic nanofiltration membrane for desalination and water treatment. *Desalination*. 2004;168(1):215-21. <https://doi.org/10.1016/j.desal.2004.07.001>
7. Han J, Cho YH, Kong H, Han S, Park HB. Preparation and characterization of novel acetylated cellulose ether (ACE) membranes for desalination applications. *J Membr Sci*. 2013;428(1):533-45. <https://doi.org/10.1016/j.memsci.2012.10.043>
8. Xu F, Chen S, You M, Meng J. Water and salt transport properties of zwitterionic poly (arylene ether ketone) for desalination membrane applications. *J Membr Sci*. 2023;687(1):122055. <https://doi.org/10.1016/j.memsci.2023.122055>
9. Guo Q, Huang Y, Xu M, Huang Q, Cheng J, Yu S, et al. PTFE porous membrane technology: A comprehensive review. *J Membr Sci*. 2002;664(1):121115. <https://doi.org/10.1016/j.memsci.2022.121115>
10. Wang N, Wang X, Ding B, Yu J, Sun G. Tunable fabrication of three-dimensional polyamide-66 nano-fiber/nets for high efficiency fine particulate filtration. *J Mater Chem*. 2012;22(1):1445-52. <https://doi.org/10.1039/C1JM14299B>
11. Hu Y, Cheng Y, Zhang X, Huang D, Chen W, Duan M. In-situ thermal crosslinked PA66/β-cyclodextrin/PA66 nanofibrous membranes with high mechanical strength for removal of heavy metal ions by flow through adsorption. *Poly Test*. 2020;91(1):106854. <https://doi.org/10.1016/j.polymertesting.2020.106854>
12. Gao SL, Qiu JK, Xu ZL, Lian C, Liu HL, Li JH, et al. Comparative analysis of polyamide nanofiltration membranes resistance to different acids: Insights from experiments and density functional theory simulations. *J Membr Sci*. 2024;694(1):122412. <https://doi.org/10.1016/j.memsci.2024.122412>
13. Karche T. The application of hemp (*Cannabis sativa* L.) for a green economy: A review. *Turkish J Botany*. 2019;43(1):710-23. <https://doi.org/10.3906/bot-1907-15>
14. Krüger M, Van Eeden T, Beswa D. *Cannabis sativa* cannabinoids as functional ingredients in snack foods-History. *Develop Aspec Plants*. 2022;1:3330. <https://doi.org/10.3390/plants1123330>
15. Andre CM, Hausman JF, Guerriero G. *Cannabis sativa*: the plant of the thousand and one molecules. *Front Plant Sci*. 2016;7(1):174167. <https://doi.org/10.3389/fpls.2016.00019>
16. Zimniewska M. Hemp fibre properties and processing target textile: A review. *Materials*. 2022;15(1):1901. <https://doi.org/10.3390/ma15051901>
17. Zhao J, Xu Y, Wang W, Griffin J, Roozeboom, K. Bioconversion of industrial hemp biomass for bioethanol production: A review. *Fuel*. 2020;281(1):118725. <https://doi.org/10.1016/j.fuel.2020.118725>
18. Ji A, Jia L, Kumar D, Yoo CG. Recent advancements in biological conversion of industrial hemp for biofuel and value-added products. *Fermentation*. 2021;7(1):6. <https://doi.org/10.3390/fermentation7010006>
19. Pakarinen A, Zhang J, Brock T, Maijala P, Viikari L. Enzymatic accessibility of fiber hemp is enhanced by enzymatic or chemical removal of pectin. *Bioresour Technol*. 2012;107(1):275-81. <https://doi.org/10.1016/j.biortech.2011.12.101>
20. Islam MS, Mccutcheon JR, Rahaman MS. A high flux polyvinyl acetate-coated electrospun nylon 6/SiO₂ composite microfiltration membrane for the separation of oil-in-water emulsion with improved antifouling performance. *J Membr Sci*. 2017;537(1):297-309. <https://doi.org/10.1016/j.memsci.2017.05.019>
21. Yin J, Zhou J. Novel polyethersulfone hybrid ultrafiltration membrane prepared with SiO₂-g-(PDMAEMA-co-PDMAPS) and its antifouling performances in oil-in-water emulsion application. *Desalination*. 2015;365(1):46-56. <https://doi.org/10.1016/j.desal.2015.02.017>
22. He M, Fan X, Yang Z, Zhang R, Liu Y, Fan L, et al. Antifouling high-flux membranes via surface segregation and phase separation controlled by the synergy of hydrophobic and hydrogen bond interactions. *J Membr Sci*. 2016;520(1):814-22. <https://doi.org/10.1016/j.memsci.2016.08.044>
23. Ding C, Zhang M, Lyu B, Guo Z, Xing N, Pang X, et al. Micropore engineering of polyamide loose nanofiltration membrane for efficient dye/salt separation. *J Membr Sci*. 2024;705:122932. <https://doi.org/10.1016/j.memsci.2024.122932>
24. Li B, Qu C, Wang S, Yeo JCC, Surat'man NEB, Loh XJ, et al. Closed-loop recyclable dynamic covalent crosslinked nanofibrous membranes for efficient oil/water separation. *J Membr Sci*. 2024;693(1):122378. <https://doi.org/10.1016/j.memsci.2023.122378>
25. Ma W, Ding Y, Li Y, Gao S, Jiang Z, Cui J, et al. Durable, self-healing superhydrophobic nanofibrous membrane with self-cleaning ability for highly-efficient oily wastewater purification, *J Membr Sci*. 2021;634(1):119402. <https://doi.org/10.1016/j.memsci.2021.119402>
26. Zhang J, Fang W, Zhang F, Gao S, Guo Y, Li J, et al. Ultrathin microporous membrane with high oil intrusion pressure for effective oil/water separation. *J Membr Sci*. 2020;608(1):118201. <https://doi.org/10.1016/j.memsci.2020.118201>
27. Zhang J, Fang W, Zhang F, Gao S, Guo Y, Li J, et al. Zwitterionic cyclodextrin membrane with uniform subnanometre pores for high-efficient heavy metal ions removal. *J Membr Sci*. 2023;688(1):122123. <https://doi.org/10.1016/j.memsci.2023.122123>
28. Emadzadeh D, Lau WJ, Matsuura T, Rahbari-Sisakht M, Ismail AF. A novel thin film composite forward osmosis membrane prepared from PSf-TiO₂ nanocomposite substrate for water desalination. *Chem Eng J*. 2014;237(1):70-80. <https://doi.org/10.1016/j.cej.2013.09.081>
29. Mouro C, Gomes AP, Gouveia IC. From hemp waste to bioactive nanofiber composites: deep eutectic solvents and electrospinning in upcycling endeavors, *Gels*. 2023;10(1):203. <https://doi.org/10.3390/gels10010001>
30. Bhattarai N, Edmondson D, Veiseh O, Matsen FA, Zhang M. Electrospun chitosan-based nanofibers and their cellular compatibility. *Biomaterials*. 2005;26(1):6176-84. <https://doi.org/10.1016/j.biomaterials.2005.03.027>
31. Erbasti UY, Candan I, Gündoğdu Y, Gümgüm HB, Kılıç HS. Investigation of PAN: hemp stems nanofibers produced by electrospinning method. *Int J Pure Appl Sci*. 2022;8(1):331-41. <https://doi.org/10.29132/ijpas.1092339>
32. Goroškaitė S. The formation and analysis of electrospun materials from nano-microfibers with hemp extract. [PhD Thesis]. Kauno Technologijos Universitetas; 2020.
33. Xia S, Yao L, Zhao Y, Li N, Zheng Y. Preparation of graphene oxide modified polyamide thin film composite membranes with improved hydrophilicity for natural organic matter removal. *Chem Eng J*. 2015;280(1):720-7. <https://doi.org/10.1016/j.cej.2015.06.063>
34. Yang Z, Shen C, Zou Y, Wu D, Zhang H, Chen K. Application of solution blow spinning for rapid fabrication of gelatin/nylon 66 nanofibrous film. *Foods*. 2021;10(1):2339. <https://doi.org/10.3390/foods10102339>

35. Chi E, Tang Y, Wang Z. In situ SAXS and WAXD investigations of polyamide 66/reduced graphene oxide nanocomposites during uniaxial deformation. *ACS Omega*. 2021;6(1):11762-71. <https://doi.org/10.1021/acsomega.1c01365>

36. Zhang H, Li S, White CJB, Ning X, Nie H, Zhu L. Studies on electrospun nylon-6/chitosan complex nanofiber interactions. *Electrochim Acta*. 2009;54(1):5739-45. <https://doi.org/10.1016/j.electacta.2009.05.021>

37. Karam L, Jama C, Mamede AS, Boukla S, Dhuister P, Chihib NE. Nisin-activated hydrophobic and hydrophilic surfaces: assessment of peptide adsorption and antibacterial activity against some food pathogens. *Appl. Microbiol Biotechnol*. 2013;97(24):10321-8. <https://doi.org/10.1007/s00253-013-5259-1>

38. Lin SL, Hsiao WC, Jee SH, Yu HS, Tsai TF, Lai JY, et al. Study on the effects of nylon-chitosan-blended membranes on the spheroid-forming activity of human melanocytes. *Biomaterials*. 2006;27(1):5079-88. <https://doi.org/10.1016/j.biomaterials.2006.05.035>

39. Niu X, Qin M, Xu M, Zhao L, Wei Y, Hu Y, et al. Coated electrospun polyamide-6/chitosan scaffold with hydroxyapatite for bone tissue engineering. *Biomed Mater*. 2021;16(1):025014. <https://doi.org/10.1088/1748-605X/abd68a>

40. Acarer S, Pir I, Tüfekci M, Türkoğlu Demirkol G, Tüfekci N. Manufacturing and characterisation of polymeric membranes for water treatment and numerical investigation of mechanics of nanocomposite membranes. *Polymers*. 2021;13(1):1661. <https://doi.org/10.3390/polym13101661>

41. Rana D, Matsuura T. Surface modifications for antifouling membranes. *Chem Rev*. 2010;110(1):2448-71. <https://doi.org/10.1021/cr800208y>

42. Xu C, Chen W, Gao H, Xie X, Chen Y. Cellulose nanocrystal/silver (CNC/Ag) thin-film nanocomposite nanofiltration membranes with multifunctional properties. *Environ Sci Nano*. 2020;(7):803-16 <https://doi.org/10.1039/C9EN01367A>

43. He G, Kong Y, Zheng H, Ke W, Chen X, Yin Y, et al. Preparation and properties of poly (amidoamine) dendrimer/quaternary ammonium chitosan hydrogels. *Journal of Wuhan University of Technology-Mater Sci Ed*. 2018;33(3):736-43. <https://doi.org/10.1007/s11595-018-1886-9>

44. Mrad H, Alix S, Migneault S, Koubaa A, Perré P. Numerical and experimental assessment of water absorption of wood-polymer composites. *Measurement*. 2018;115:197-203. <https://doi.org/10.1016/j.measurement.2017.10.011>

45. Rajesh G, Prasad AR, Gupta AVSSKS. Mechanical and degradation properties of successive alkali treated completely biodegradable sisal fiber reinforced poly lactic acid composites. *J Reinf Plast Compos*. 2015;34(12):951-61. <https://doi.org/10.1177/0731684415584784>

Additional information

Peer review: Publisher thanks Sectional Editor and the other anonymous reviewers for their contribution to the peer review of this work.

Reprints & permissions information is available at https://horizonpublishing.com/journals/index.php/PST/open_access_policy

Publisher's Note: Horizon e-Publishing Group remains neutral with regard to jurisdictional claims in published maps and institutional affiliations.

Indexing: Plant Science Today, published by Horizon e-Publishing Group, is covered by Scopus, Web of Science, BIOSIS Previews, Clarivate Analytics, NAAS, UGC Care, etc
See https://horizonpublishing.com/journals/index.php/PST/indexing_abstracting

Copyright: © The Author(s). This is an open-access article distributed under the terms of the Creative Commons Attribution License, which permits unrestricted use, distribution and reproduction in any medium, provided the original author and source are credited (<https://creativecommons.org/licenses/by/4.0/>)

Publisher information: Plant Science Today is published by HORIZON e-Publishing Group with support from Empirion Publishers Private Limited, Thiruvananthapuram, India.